

A 2D Improvement of Radiative Heat Transfer with the P1 Approximation and a Statistical Narrow Band Model

A. Khourchafi¹, M. El Alami^{2,3}, M. Najam² and M. Belhaq⁴

Abstract: A spectral radiation study has been carried out in the framework of a statistical narrow-band model based on an inverse-tailed exponential law and the so-called P1 approximation. This new spectral formulation, which may be also regarded as a grey band formulation with a local absorption coefficient, leads to two implementation methods: a non correlated form in which the averaged formulation of the P1 approximation does not take into account the correlation between fundamental quantities and a pseudo-correlated variant consisting basically of a technique for improving the anisotropy of the radiative intensity. Real gases (H₂O, CO₂) are considered. The resulting tests show the limitation of the method in radiative heat transfer. A proper consideration of the spectral correlation with the technique of the correlation “indicator”, however, leads to an appreciable increase of the accuracy. Since the thermal discontinuity near the corners is known to penalize the P1 method, it is expected that the present formulation may give even better results in more general cases (for which the sharpness of thermal gradients near the walls is less pronounced).

Keywords: Radiative heat transfer, P-N Methods, infrared gas, Statistical Narrow-Band models, CFD.

¹ Equipe de Recherche Appliquée sur les Polymeres, Ecole Nationale Supérieure d'Electricité et de Mécanique (ENSEM), Université Hassan II Aïn Chock, Km 8 Route d'El Jadida-BP: 8118 - Maârif Casablanca, Morocco

² Groupe de Thermique, Département de physique, Faculté des Sciences, Université Hassan II Aïn Chock, Km 8 Route d'El Jadida-BP: 5366 - Maârif Casablanca, Morocco

³ Corresponding author: m.elalami@fsac.ac.ma; elalami_m@hotmail.com

⁴ Laboratoire de Mécanique, Faculté des Sciences, Université Hassan II Aïn Chock, Km 8 Route d'El Jadida-BP: 5366 - Maârif Casablanca, Morocco

Nomenclature

C	optical path length	Greek symbols
$C(\vec{r}, \vec{u})$	correlation coefficient	k, β band model parameters
E_y, E_z	enclosure dimensions [m]	ε emissivity
I	total radiation intensity [$\text{W}/\text{m}^2 \cdot \text{sr}$]	ν wave number [cm^{-1}]
I_ν	spectral radiation intensity [$\text{W} \cdot \text{cm} / \text{m}^2 \cdot \text{sr}$]	$\Delta\nu$ band width [cm^{-1}]
I^b	Blackbody intensity [$\text{W}/\text{m}^2 \cdot \text{sr}$]	τ transmissivity
L_m	local mean path length [m]	$\bar{\kappa}_\nu$ narrow band averaged absorption coefficient [m^{-1}]
M_0	zero th moment of radiative intensity	
p	total pressure [atm]	Subscripts
P^R	radiative source term [W/m^3]	C correlated quantities
\vec{q}^R	radiative flux vector [W/m^2]	c cold wall
\vec{q}^{R*}	dimensionless radiative flux vector	h hot wall
S	local surface area of a control volume [m^2]	p parietal quantities
T	temperature [$^\circ\text{K}$]	NC non-correlated quantities
\vec{u}	unitary vector of an elementary solid angle	ν spectral quantities
$\vec{u}(\theta, \varphi)$		Superscripts
V	computational control volume [m^3]	Properties averaged over the band width $\Delta\nu$
x_i	molar fraction of species i	
x, y, z	cartesian coordinates [m]	

1 Introduction

Development of accurate and efficient non-grey gas radiation models is important in many engineering applications including a variety of flame and combustion devices (mainly industrial furnaces) and heat recovery industrial plants. In general, the performance of such systems is known to depend on the related phenomena of radiative heat transfer from the hot combustion products (mainly H_2O , CO_2 and CO) and the turbulent convective heat transfer which occurs in the gas flow at high temperature.

The level of detail required for the analysis of such a subject depends essentially on the fundamental mechanisms to be investigated (which include: the instantaneous spectral local radiative flux, flame structure, scalar properties of the flame, formation of flame-generated particles, local radiative flux and its divergence or the temperature distribution).

For example, when a model is used to predict pollutant concentrations, accurate temperatures are of great importance since the chemical kinetics involved are extremely temperature dependent. In many circumstances, radiation heat transfer can be considered as the dominant mode of transfer. Unfortunately, radiative heat transfer is governed by a complex integro-differential equation that is time consuming to

solve. For this reason, achieving a good compromise between an efficient method of solution and an acceptable level of accuracy is not an easy task.

For engineering radiative heat transfer calculations, where absorption emitting and scattering are important, accurate radiative transfer methods have been developed in the literature: The discrete transfer method (DTM) [Lockwood and Shah (1981)], the discrete ordinates method (S_N -approximation) (DOM) [Khalil and Truelove (1977); Kim and Menart (1991)], the finite volume method (FVM) [Raithby and Chui (1990); Guedri and Abbassi (2009)] and spherical harmonic (P_N -approximation) method [Modest and Sikka (1992); Yang and Modest (2007)]. A comprehensive summary of various methods has been given by Modest (2003). The lowest order spherical harmonic method, called the P1 approximation [Ratzel and Howell (1983)], was widely used in coupled problems [Klason and Bai (2007); Krishnamoorthy et al. (2006)].

The main advantage of the P1 approximation is that it reduces the Radiative Transfer Equation (RTE) to a simple elliptic partial differential equation that can be easily handled in a multi-dimensional CFD code with a relatively small additional cost [Klason and Bahador (2007); Yang and Modest (2007)]. Along these lines, Morvan et al. (2001) have performed numerical simulations of pool fires with the P1 radiation model, producing results which compare favourably with experimental results.

However, the P1 method can be accurate only in optically moderate and thick media and in the situation of scattering media where the diffusion mode is predominant. Moreover, the method lacks the knowledge of proper boundary conditions [Marshak (1949)] although its accuracy might be improved when an optimized boundary condition is used [Liu and Swithenbank (1992)]. In essence, regardless to the level of precision, the advantage of this method is the low computational time required, especially in combined transfer modes (conduction–turbulent convection and radiation).

A new formulation of the PN-approximation and its boundary conditions was proposed by Yang [Yang and Modest (2007)]. In this formulation boundary conditions are formulated in terms of local spherical harmonics and guarantee that complex geometries can be dealt without a need to develop geometry-specific boundary conditions (which is also a serious problem for the PN approximation).

On the other hand, accurate modelling of radiative heat transfer also necessitates accurate estimation of radiative properties, especially when dealing with real gases. The Narrow Band models are in general capable of providing accurate band averaged gas transmissivities and hence represent a good compromise between accuracy and computational efficiency for engineering applications where total radia-

tive quantities are needed. However, they have been not widely used mainly for the two following reasons. First, Band models provide a band spectral averaged transmissivity rather than a gas absorption coefficient [Goody (1964)] which cannot be handled directly in most differential approximation methods of the RTE (with the exception of Monte Carlo method (MC) and the discret transfer method (DTM)).

If we want to use an absorption coefficient that has been averaged over a spectral band, the RTE needs to be modified. This leads to the need to reformulate the RTE in terms of an averaged transmissivity differentiated with respect to distance in order to account for the correlation between intensity and the absorption coefficient. This rigorous form, which is very time consuming in multidimensional situations [Kim and Menart (1991); Liu, Gülder and Smallwood (1998)], requires also the specification of a path length throughout the computational domain. Secondly, the rigorous implementation of a band model into the RTE, when using a method of solution (SN, PN, DOM, DTM), leads to a correlation term between the spectral gas absorption coefficient and the others spectral fundamental quantities (mainly the radiation intensity or its moments). This complicates significantly the band averaged formulation of the RTE [Soufiani and Taine (1987); Zhang et al. (1988)].

A grey band formulation of radiative transfer in high temperature real gases is developed in this study. In order to overcome the difficulties associated with the implementation of a narrow band model into a differential approximation (P1) of the RTE, two approximate implementation methods are presented. A non correlated form resulting from a spectral averaged form of the P1 equations in which correlations are neglected between fundamental quantities, and then a pseudo-correlated variant aimed at improving the anisotropy of the intensity field with the technique of the “correlation indicator” [Zhang et al. (1988)].

2 Radiative heat transfer model

The P1 approximation radiation model, described in detail by Ratzel and Howell (1983) is employed in the present radiative heat transfer simulation. In the general case of 3D geometry, for a semi-transparent, emitting, absorbing and no scattering medium, the wavenumber-averaged P1 equations over a width of a spectral band are obtained by applying the operator spectral average defined by:

$$\overline{f_{\nu}} = \frac{1}{\Delta\nu} \int_{\Delta\nu} f_{\nu} d\nu \quad (1)$$

where f_{ν} is any monochromatic function.

The averaged P1 approximation equations are given in terms of the zeroth order

moment $M_{0,v}$ (i.e incident radiation) of the radiative intensity:

$$\sum_{j=1}^3 - \frac{\partial}{\partial x_j} \left(\frac{1}{\kappa_v(\vec{r})} \frac{\partial M_{0,v}}{\partial x_j}(\vec{r}) \right) + 3 \overline{\kappa_v(\vec{r})} M_{0,v}(\vec{r}) = 12 \pi \overline{\kappa_v(\vec{r})} \overline{I_v^b}(\vec{r}) \quad (2)$$

$M_{0,v}$, is the zeroth moment of the monochromatic intensity defined by:

$$M_{0,v}(\vec{r}) = \int_{4\pi} I_v(\vec{r}, \vec{u}) d\Omega \quad (3)$$

κ_v is the monochromatic absorption coefficient.

The averaged radiative intensity over a band width Δv is then given by:

$$\overline{I_v}(\vec{r}, \vec{u}) = \frac{1}{4\pi} \left[\overline{M_{0,v}}(\vec{r}) - \frac{1}{\kappa_v(\vec{r})} \vec{\nabla} M_{0,v}(\vec{r}) \cdot \vec{u} \right] \quad (4)$$

$$\vec{r} = \vec{r}(x, y, z) \quad \vec{u} = \vec{u}(\theta, \phi)$$

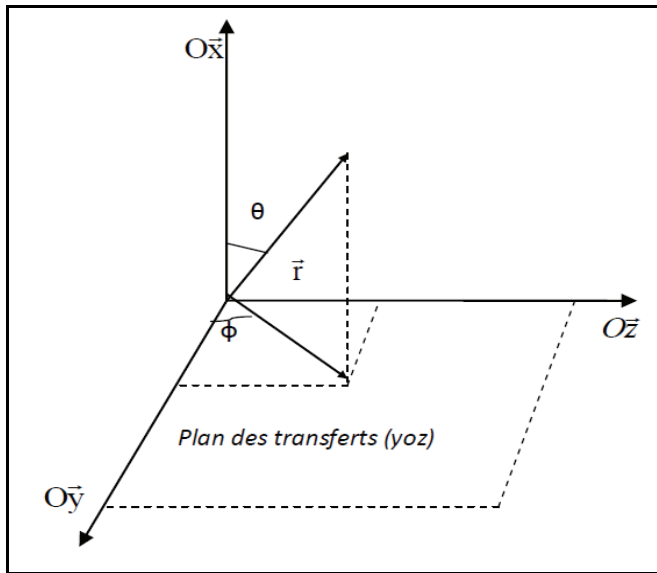


Figure 1: Schematic definition of transfer plan.

The terms (I) and (II) in equation (2) cannot be evaluated explicitly since special attention is required by the spectral correlation between the monochromatic fundamental quantities. The term (III) does not introduce any problem in this regard as

in the narrow band models the width of a spectral band is defined as that making the equilibrium radiative intensity I_ν^b , given by the Planck function, constant over the bandwidth [Young (1977)].

3 The real-gas radiative properties

The statistical Narrow Band Model (SNBM) is used in the present study to calculate the narrow band averaged gas transmissivity. The SNBM had been described in detail by [Young (1977)], [Goody (1989)] and [Soufiani et al. 1997]. Various SNB models have been tested with a line by line calculation for coupled conducting and radiating CO₂-H₂O-air mixtures. The most accurate results were obtained with the narrow band model with an exponential-tailed-inverse probability distribution of lines intensities. For a non isothermal and/or inhomogeneous medium, the Curtis-Godson approximation [Young (1977)] is used. This method approximates the nonisothermal and inhomogeneous medium, for a gas species i , with an equivalent isothermal and homogeneous medium. For usual systems in combustion, when pressure gradients are moderate, this approximation leads to very accurate results. In this case the equivalent transmissivity is given by:

$$\bar{\tau}_{\nu,CG}^i = \exp \left[-\frac{\bar{\beta}_{CG}}{\pi} \left(\sqrt{1 + \frac{2\pi \bar{k}_{CG} C}{\bar{\beta}_{CG}}} - 1 \right) \right] \quad (5)$$

Where \bar{k}_{CG} and $\bar{\beta}_{CG}$ are the equivalent parameters of Curtis Godson (CG) approximation obtained by averaging the band parameters over the optical path C for the species ' i ' [Young (1977)]:

$$C = \int_{s'}^s x_i(s'') p(s'') ds'' \quad (6)$$

$$\bar{k}_{CG} = \frac{1}{C} \int_{s'}^s x_i(s'') p(s'') \bar{k}(s'') ds'' \quad (7)$$

$$\bar{\beta}_{CG} = \frac{1}{C \bar{k}_{CG}} \int_{s'}^s x_i(s'') p(s'') \bar{k}(s'') \bar{\beta}(s'') ds'' \quad (8)$$

where $p(s)$ and $x_i(s)$ are respectively the total pressure and the molar concentration of the absorbing species ' i '; \bar{k} and $\bar{\beta}$ are the band model parameters which take into account the spectral structure of the gas.

The spectrum is subdivided into narrow bands of width $\Delta\nu$ equal to 25 cm⁻¹. For each band, the averaged effective absorption coefficient is derived from the definition of averaged transmissivity:

$$\bar{\tau}_\nu(s',s) = \exp \left(-\int_{s'}^s \kappa_\nu(s'') ds'' \right) \quad (9)$$

When absorption by different gas species occurs inside the same spectral range $\Delta\nu$, and for sake of simplicity, these difficult phenomena should be considered as not correlated, so, the transmissivity of the mixture medium is then the product of transmissivities of each species [Goody (1989)].

The derivative of the average transmissivity (9) with respect to s' taken at the point $s'=s$ leads to a rigorous expression of the averaged effective absorption coefficient which is needed in the averaged P1 equations (see equation (11)) as :

$$\bar{\kappa}_V(s) = \frac{\partial \bar{\tau}_V(s' = s, s)}{\partial s'} = \frac{1}{\Delta\nu} \int_{\Delta\nu} \kappa_V(s) d\nu \tag{10}$$

Based on a previous work [Liu, Gülder and Smallwood (1998)] an equivalent path independent narrow band averaged local absorption coefficient is estimated using the mean local path length L_m issued from the local computational control volume, $L_m = \frac{3.6V}{S}$, where V and S are the geometric characteristic of the computational control volume.

The updated SNB model parameters are provided by Soufiani et al. (1985). The data set contains SNB model parameters for CO₂, H₂O and CO with a constant spectral interval of 25 cm⁻¹. The covered temperature and spectral ranges are 300 to 2000 °K and 150 to 6000 cm⁻¹. Figure (2) represents a synthesized spectrum of absorption computed from this data set.

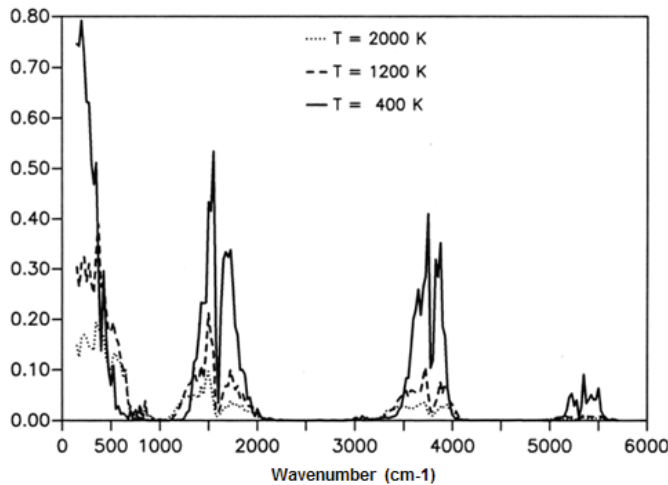


Figure 2: Example of calculated Absorptivity spectra of an isothermal column (Width E=10 cm) of pure H₂O vapor for different levels of temperature.

3.1 P1 non-correlated model

The main difficulty in real gas radiative transfer treatment is to calculate the spectral correlated terms in equations (2) and (4). In a first approach we assume that the monochromatic fundamental quantities in equation (2) are not correlated leading for each spectral band width to solve an elliptic equation in terms of the zeroth moment (i.e. incident radiation) of the radiative intensity. For radiative properties, as mentioned above, the transmissivity of the gas mixture is the product of those related to each species (case of overlapping bands of CO₂ and H₂O mixture). For a 2D rectangular cavity of dimensions (E_y, E_z) we have the following system [Khourchafi 1994]:

$$-\frac{\partial}{\partial y} \left(\frac{1}{\bar{\kappa}_v(\vec{r})} \frac{\partial \bar{M}_{0,v}(\vec{r})}{\partial y} \right) - \frac{\partial}{\partial z} \left(\frac{1}{\bar{\kappa}_v(\vec{r})} \frac{\partial \bar{M}_{0,v}(\vec{r})}{\partial z} \right) + 3 \bar{\kappa}_v(\vec{r}) \bar{M}_{0,v}(\vec{r}) = 12 \pi \bar{\kappa}_v(\vec{r}) \bar{I}_v^b(\vec{r}) \quad (11)$$

The Marschak's boundary [Marschak (1949)] conditions associated are:

$$\mp h(\varepsilon_p) \frac{1}{\bar{\kappa}_v} \frac{\partial \bar{M}_{0,v}}{\partial y} + \bar{M}_{0,v} = 4 \pi \bar{I}_v^b \quad (12)$$

at $y = 0$ and $y = E_y$.

$$\mp h(\varepsilon_p) \frac{1}{\bar{\kappa}_v} \frac{\partial \bar{M}_{0,v}}{\partial z} + \bar{M}_{0,v} = 4 \pi \bar{I}_v^b \quad (13)$$

at $z = 0$ and $z = E_z$.

$h(\varepsilon_p) = \frac{2}{3} \frac{2-\varepsilon_p}{\varepsilon_p}$, where ε_p is the emissivity at the correspondent wall.

Assuming two-dimensionality of radiative transfer ($q_x^R = 0$) (see fig. 1) the expression of noncorrelated directional radiative intensity, for a spectral band, given by (4), is simplified ($\theta = \frac{\pi}{2}$). It is given in the (y, z) plan by:

$$\bar{I}_v^{NC}(\vec{r}, \vec{u}) = \frac{1}{4\pi} \left(\bar{M}_{0,v}(\vec{r}) - \frac{1}{\bar{\kappa}_v(\vec{r})} \left(\cos(\phi) \frac{\partial \bar{M}_{0,v}(\vec{r})}{\partial y} + \sin(\phi) \frac{\partial \bar{M}_{0,v}(\vec{r})}{\partial z} \right) \right) \quad (14)$$

The components of the radiative heat flux and the radiative dissipation for each band are given by:

$$\vec{q}_{v,j}^R(\vec{r}) = -\frac{1}{3\bar{\kappa}_v(\vec{r})} \frac{\partial \bar{M}_{0,v}(\vec{r})}{\partial x_j} \quad (j = 1, 2) \quad (15)$$

$$\bar{P}_v^R(\vec{r}) = -\text{Div}(\vec{q}_v^R) = \bar{\kappa}_v(\vec{r}) \left(\bar{M}_{0,v}(\vec{r}) - 4 \pi \bar{I}_v^b(\vec{r}) \right) \quad (16)$$

The total quantities are computed by summing over the spectrum:

$$\vec{q}_j^R(\vec{r}) = \sum_{spectrum} -\frac{1}{3\bar{\kappa}_v(\vec{r})} \frac{\partial \bar{M}_{0,v}(\vec{r})}{\partial x_j}$$

$$\bar{P}^R(\vec{r}) = -Div(\vec{q}^R)$$

3.2 Correlated P1 formulation

We have seen that the approximations (described in 2.2) necessary for coupling the P1 to the narrow bands model does not account for the effects of spectral correlations and lead to a radiative intensity called non-correlated. A simple way to overcome this error is to introduce a correlation factor $C(\vec{r}, \vec{u})$ which allows approximating the correlated intensity I_v^C in the same manner as well done by Zhang [Zhang et al. (1988)]:

$$\bar{I}_v^C(\vec{r}, \vec{u}) = C_v(\vec{r}, \vec{u}) \bar{I}_v^{NC}(\vec{r}, \vec{u}) \tag{17}$$

In the general case, $C_v(\vec{r}, \vec{u})$ is calculated in the six principal directions $\pm \vec{u}_i$ ($i = 1, 2, 3$) corresponding to the coordinate axis and thus for each band. The Curtis Godson approximation is associated to a discrete direction method for approximating the RTE is used to calculate the exact correlated intensity $\bar{I}_v^C(\vec{r}, \pm \vec{u}_i)$. In a 2D configuration, the correlation coefficient is approximated by Zhang [Zhang et al. (1988)]:

$$C_v(\vec{r}, \pm \vec{u}_i) = \left[(C_{1,v}(\vec{r}, \pm \vec{u}_i) \cos \phi)^2 + (C_{2,v}(\vec{r}, \pm \vec{u}_i) \sin \phi)^2 \right]^{1/2} \tag{18}$$

From the correlated intensity field, radiative flux and radiative power are calculated, for each band:

$$\vec{q}_v^R(\vec{r}) = \int_{4\pi} C_v(\vec{r}, \vec{u}) \bar{I}_v^{NC}(\vec{r}, \vec{u}) \vec{u} d\Omega \tag{19}$$

$$\bar{P}_v^R(\vec{r}) = -\vec{\nabla} \cdot \vec{q}_v^R(\vec{r}) \tag{20}$$

Typically in the case of combustion gases, in [300, 2000°K] range, 173 of H₂O bands and 73 bands of CO₂ are considered in our calculations. The band parameters are provided from reference [Soufiani et al. (1985)] as mentioned above.

3.3 Method of solution

In order to incorporate further the method in a CFD approach, equation (11) associated with the Marshak's boundary conditions (12) and (13) are formulated in terms of a finite volume formulation. The non linear elliptic equation obtained is discretized using a second order central difference schemes for the spatial derivatives, applied in the control volume centre. The computations were performed with a (41x41) uniform grid in the case of the gray gas and a (61x91) non uniform grid in the case of real gas . Special attention was devoted to the calculation of the local absorption based length path coefficient. For more details see [Khourchafi, 1994].

The calculation procedure is simple: starting with a specified field of gas temperature and a given composition of the mixture, our code solves the RTE by the P1 approximation, for each band. Then, we calculate the spectral radiative heat flux and spectral radiative power. Finally we determine the total quantities by summing over the spectrum. This scenario leads to the generation of benchmark solutions of radiative heat transfer.

4 Results

4.1 Grey gas assessment

Before considering radiative transfer in the case of real gases, a grey gas test validation is considered. The test case is a gray medium confined in a square geometry ($E_y=E_z=1\text{m}$) with black walls ($(\epsilon_p(i) = 1 (i = 1,4))$). The bottom, left and right walls are at a fictive temperature $T_c = 0\text{ K}$ while the hot wall (wall 1) is at a temperature $T_h = 1000\text{ K}$. The absorption coefficient of the gas is chosen so that the optical thickness is equal to unity in the two main directions of transfer [Ratzel and Howell 1983].

Figures (3) and (4) show an excellent agreement with the Ratzel P1 model. We note that the P1 model overestimate the radiative heat flux than the zone method and P3 approximation. Two intrinsic behavior of the P1 model are noted. First the error is large near the corner where the anisotropy of the intensity is large. We note, because the higher order of truncation in the spherical harmonics series, the P3 model matches more this anisotropy. Secondly the error is smaller when the wall emissivity decreases marking, then, a less anisotropy of the intensity field.

4.2 Real gas analysis

We present numerical solutions obtained using the correlated and non-correlated models, in the case of a real infrared-active gas like H_2O , with a spectral resolution $\Delta\nu = 25\text{cm}^{-1}$. The calculations have been done in the case of a rectangular

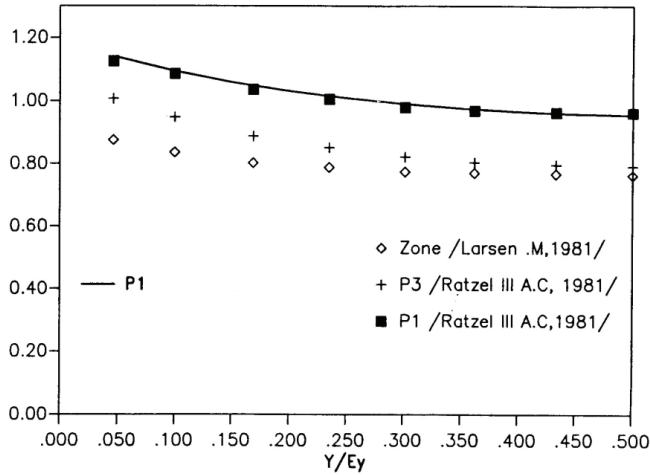


Figure 3: Non-dimensional radiative heat flux $\vec{q}^{R*} = \frac{\vec{q}^R}{\sigma T_h^4}$; hot wall; ($\epsilon_p(i) = 1$)

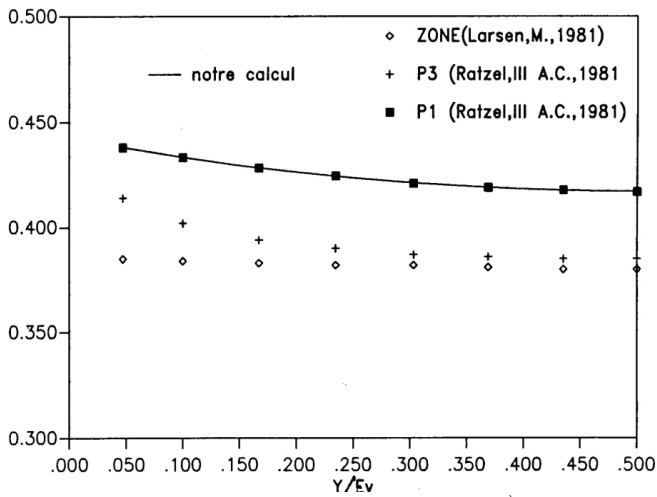


Figure 4: Non-dimensional radiative heat flux $\vec{q}^{R*} = \frac{\vec{q}^R}{\sigma T_h^4}$; hot wall; ($\epsilon_p(i) = 0.5$).

cavity of dimensions $E_y=1\text{m}$ and $E_z = 0.40\text{ m}$) containing pure water vapor. Computations were made for different concentrations of H_2O , simulating the opacity of the medium. The water vapor is taken at a constant temperature equal to 1200 K. The walls are assumed isothermal at 400 K with isotropic emission and diffuse

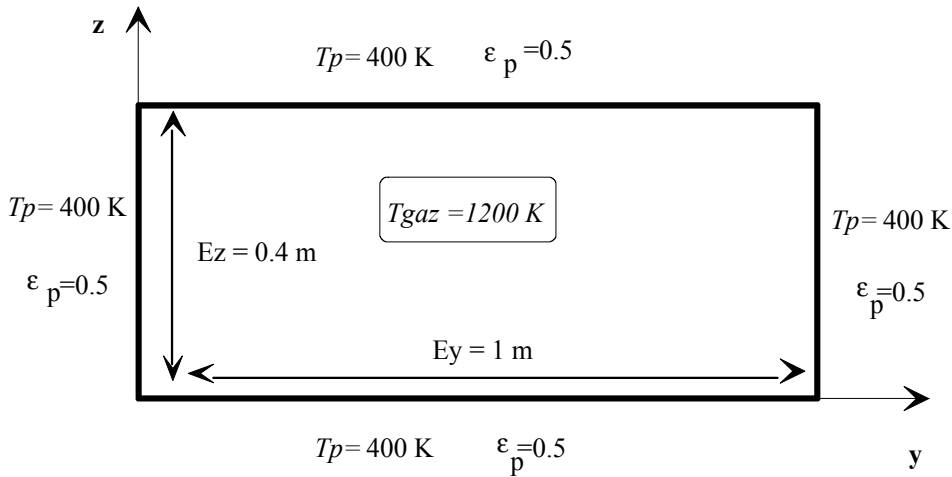


Figure 5: Definition of the test case.

reflection. The emissivity of the walls is taken equal to $\varepsilon_p = 0.5$.

Due to the symmetry of the problem, the results are presented only for the bottom and left walls. They are given only for the spectral band centred around ($\nu=3600 \text{ cm}^{-1}$) for two concentrations of water vapor $x_{H_2O} = 0.1$ and $G_{x_{H_2O}} = 0.1$. The absorption at this band is highly intense ($\bar{k} = 0.245 \text{ cm}^{-1} \cdot \text{atm}^{-1}$ and $\bar{\beta} = 3.60 \text{ cm}^{-1}$). Our computations are compared to a reference model using a discrete direction method [Zhang et al. (1988)].

This simple case is a severe test for the P1 method because it induces a large anisotropy of radiative intensity due to the sharpness of temperature gradient field, especially near the corners. It is found that heat exchange is more important at the center of walls than corners, fig.6 and 7. The radiative heat flux is more homogeneous for the bottom wall. Gradually as the concentration of water vapor decreases, which results in decreasing the optical thickness of the medium represented by the product $(p \cdot x_{H_2O} \cdot l)$, parietal transfer tends to become more uniform. It appears, referring to the overall results, that the P1 correlated method gives better agreement with the reference model than the P1 noncorrelated method because the anisotropy field luminance is improved by the technique of indicator of correlation. We note that in the case of a thick medium $x_{H_2O} = 1$ (Fig. 6 and 7), the P1 model overestimates the radiative flux in both sides of the enclosure but gives better results than the noncorrelated reference model. It should be noted that the P1 correlated model provides a great improvement in computing time compared to that used in reference [Zhang al. (1988)] (a minimum ratio of 400).

For $x_{H_2O} = 0.1$ (intermediate optical thickness) (Fig. 8 and 9) results show that the P1 models become relatively less accurate. The non-correlated P1 model overestimates by at least 20% the reference model; the maximum being observed near the corners of the geometry. Taking into account that the technique of correlation significantly improves the P1 model since it gets 5% and 9% error respectively in the centers of the bottom wall and the left one.

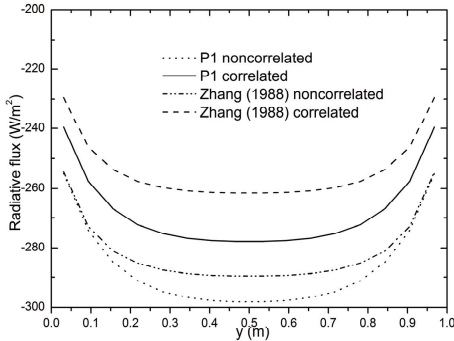


Figure 6: Distribution of radiative heat flux along the bottom wall ($x_{H_2O} = 1$, $\nu = 3600 \text{ cm}^{-1}$).

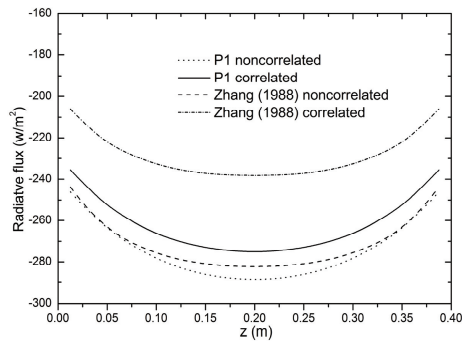


Figure 7: Distribution of radiative heat flux along the left wall ($x_{H_2O} = 1$, $\nu = 3600 \text{ cm}^{-1}$).

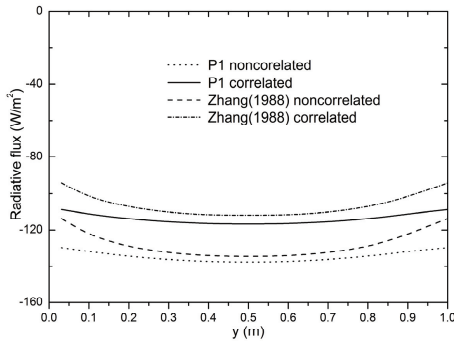


Figure 8: Distribution of radiative heat flux along the bottom wall ($x_{H_2O} = 0.1$, $\nu = 3600 \text{ cm}^{-1}$).

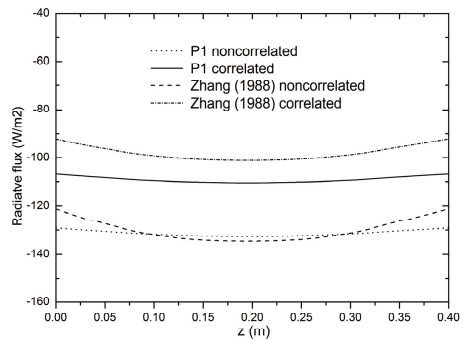


Figure 9: Distribution of radiative heat flux along the left wall ($x_{H_2O} = 0.1$, $\nu = 3600 \text{ cm}^{-1}$).

Figure (10) shows the profile (plane $z = 0.20 \text{ m}$) of radiative source term in the case of $x_{H_2O} = 1$. The P1 models over-predict the radiative source term. Here, also, the technique of “indicatrice” of correlation improves the accuracy of the spectral P1

model. However, the maximum error in the cavity does not exceed 20% for the P1 correlated model. Figure (11) presents the profile of radiative source term for $x_{H_2O}=0.1$. The error is around 32% in the center of the cavity, for the P1 correlated models. In both cases, the P1 spectral model over-predict the radiative source term.

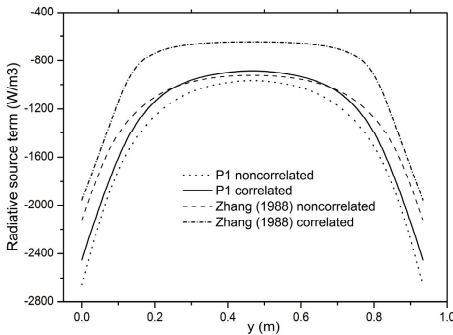


Figure 10: Predicted radiative source term; plane $z=0.2$ m, $x_{H_2O}=1$, $\nu=3600$ cm^{-1}

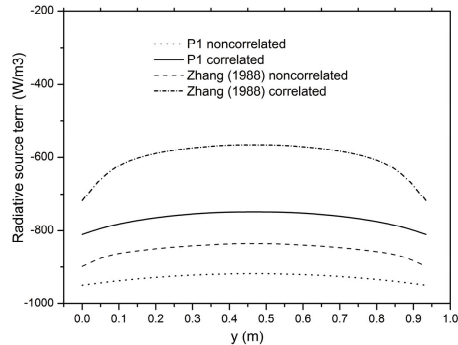


Figure 11: Predicted radiative source term; plane $z=0.2$ m, $x_{H_2O}=0.1$, $\nu=3600$ cm^{-1}

5 Conclusion

A study of radiative heat transfer in the case of a high temperature real gas in the infrared range has been conducted.

The P1 method was coupled to a statistical narrow band model with an exponential-tailed-inverse distribution law. A correction technique (called “indicator” of correlation) has been used for improving the anisotropy field of the intensity of luminance. This has led to a new grey-band formulation in a inhomogeneous emitting, absorbing and non scattering medium.

For the considered relatively simple test cases, our results have shown the classical limitations of this category of methods (in the case of gases from combustion). A proper consideration of the spectral correlation in the framework of the “indicator of correlation” technique, however, has been shown to improve greatly the resulting accuracy.

Despite the known penalization of the P1 method due to the sharpness of the temperature gradient, our model agrees relatively well with the non-correlated reference model. The objective behind this approach was to combine the method P1 to

a multidimensional computer CFD code in the case of gas flow originating from high temperature combustion.

References

- Goody R.; Yung Y. L.** (1989): *Atmospheric Radiation*. 2nd edition, Oxford Univ., UK.
- Guedri K ; Abbassi M.A.; Borjini M.N.; Halouani K.; Saïd R.**(2009) : Application of the finite volume method to study the effects of baffles on radiative heat transfer in complex enclosures. *Numerical Heat Transfer (Part A)*, vol.55, pp. 780-806.
- Khalil E. E.; Truelove J. S.** (1977): Calculations of radiative heat transfer in a large gas filled furnace. *Letters in Heat and Mass Transfer*. vol. 4, pp. 353–365.
- Khouchafi A.** (1994): Etude des transferts couples convection-rayonnement dans des échangeurs de Chaleur à haute température. *Thèse de Doctorat*, Ecole Centrale Paris, 1994.
- Kim T. K.; Menart J. A. ; Lee H. S.** (1991) : Nongray radiative gas analysis using the S-N discrete ordinates method. *ASME J. Heat Trans.* vol. 113, pp. 946-952.
- Klason T.; Bai X. S.** (2007): Computational study of the combustion process and NO formation in a small-scale wood pellet furnace. *Fuel*. vol. 86, no. 10-11, pp. 1465-1474.
- Klason T.; Bai X. S.; Bahador M.; Nilsson T. K.; Sundén B.** (2007): Investigation of radiative heat transfer in fixed bed biomass furnaces. *Fuel*, vol. 87, no. 10-11, pp. 2141-2153.
- Krishnamoorthy G.; Rawat R.; Smith P. J.** (2006): Parallelization of the P1 radiation model. *Numerical Heat Transfer, Part B*, vol. 49, pp. 1–17.
- Liu F. ; Gülder O.L.; Smallwood G.J.; Ju Y.** (1998): Non-gray gas radiative transfer analyses using the statistical narrow-band model. *Int. J. Heat Mass Transfer*, vol. 41, no. 14, pp. 2227-2236.
- Liu F.; Swithenbank J.; Garbett E. S.** (1992): The boundary condition of the PN-approximation used to solve the radiative transfer equation. *Int. J. Heat Mass Transfer*, vol. 35, pp. 2043-52.
- Lockwood F. C.; Shah N. G.** (1981): A new radiation solution method for incorporation in general combustion prediction procedures. *Proceedings of the Eighteenth International Symposium on Combustion*, pp. 1405–1413.
- Marschak R. E.** (1949): Note on the spherical harmonics method as applied to the Milne problem for a sphere. *Phys. Review*, vol. 71, p. 443.

- Modest M. F.** (2003): Radiative heat transfer. 2nd ed. United States: Academic Press.
- Modest M. F.; Sikka K.K.** (1992): The stepwise gray P1 approximation for multi-dimensional radiative transfer in molecular-gas-particulate mixtures. *J. Quant. Spectrosc. Radiat. Transfer*, vol. 48, no. 2, pp. 159-168.
- Morvan D.; Porterie B.; Loraud J. C.; and Larini M.** (2001): A numerical Investigation of Cross Wind Effects on a Turbulent Buoyant Diffusion Flame. *Combustion Sci. Technol.*, vol. 164, pp. 1–35.
- Raithby G. D.; Chui E. H.** (1990): A finite volume method for predicting a radiant heat transfer enclosure with participating media. *ASME J. Heat Transfer*, vol. 112, pp. 415-23.
- Ratzel III, A. C.** (1981): PN differential approximation of one and two dimensional radiation and conduction energy transfer in gray participating media. Ph. D. thesis, University of Texas at Austin.
- Soufiani A.; Hartmann J. M.;Taine J.** (1985): Validity of band-model calculations for CO₂ and H₂O applied to radiative properties and conductive-radiative transfer. *J. Quant. Spectrosc. Radiat. Transfer*, vol. 33, no. 3, pp.243-257.
- Soufiani A.; Taine J.** (1987): Application of statistical narrow-band model to coupled radiation and convection at high temperature. *Int. Journal of Heat and Mass Transfer*, vol. 30, p. 437.
- Soufiani A.; Taine J.** (1997): High temperature gas radiative property parameters of statistical narrow-band model for H₂, CO₂ and CO and correlated-K (CK) model for H₂O and CO₂. *Int. J. Heat Mass Transfer*, vol. 40, no. 4, pp. 987-991.
- Yang J.; Modest M.F.** (2007): Elliptic PDE formulation of general, three dimensional high-order PN-approximations for radiative transfer. *J. Quant. Spectrosc. Radiat. Transfer*, vol. 104, pp. 217–27.
- Young S. J.** (1977): Nonisothermal band theory. *J. Quant. Spectrosc. Radiat. Transfer*, vol. 18, no 2, p. 1.
- Zhang L.;Soufiani A.;Taine J.** (1988) : Spectral correlated and non-correlated radiative transfer in a finite axinsymmetric system containing an absorbing and emitting real gas-particle mixture. *Int. Journal of Heat and Mass Transfer*, vol. 31, pp. 2261–2272.